Estimation of Gravity Wave Momentum and Drag from High-Resolution Idealized Baroclinic Wave Simulations

Junhong Wei, Fuqing Zhang

Department of Meteorology
The Pennsylvania State University

Friday 15th August, 2014

Part I: Gravity Wave Overview

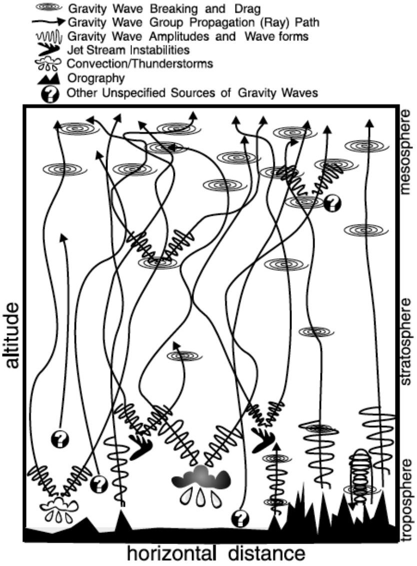

Kim et al. (Atmosphere-Ocean, 2003)

- Generation Mechanisms

Topography

Jet imbalance

Frontogenesis

Convection

Shear Instability

Density Current

- Impacts of Gravity Waves

Momentum and Energy Transport

Induce Clear-Air Turbulence

Initiation and Modulation of Convection

Part I: Shutts and Vosper (2011)

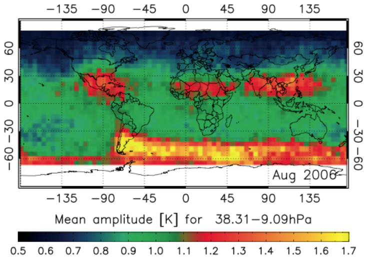

Figure 1. The global distribution of the mean temperature wave amplitude in the layer 38.3 to 9.1 hPa for August 2006 calculated from HIRDLS data. A filtering procedure has been used to isolate gravity waves with horizontal wavelengths in the approximate range 100 to 400 km. Reproduced from Yan *et al.* (2010) with permission (© American Geophysical Union).

Observation

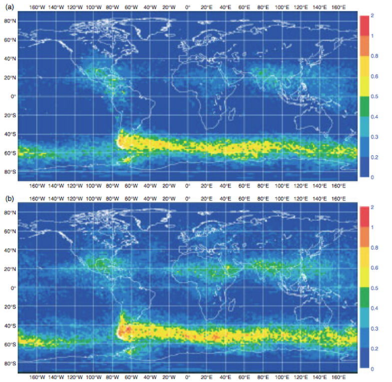

Figure 4. The monthly mean global distributions of temperature wave amplitude, $|T'|$ (K) computed from (a) the MetUM and (b) the IFS forecasts for August 2006. The data shown are for 32.3 km (MetUM) and 31.2 km (IFS) amsl and were calculated using daily forecasts valid at T+6 h. The resolution of the data is approximately 40 km.

NWP models

- The overall patterns generally match each other.

Part I: Wei and Zhang (2014, JAS)

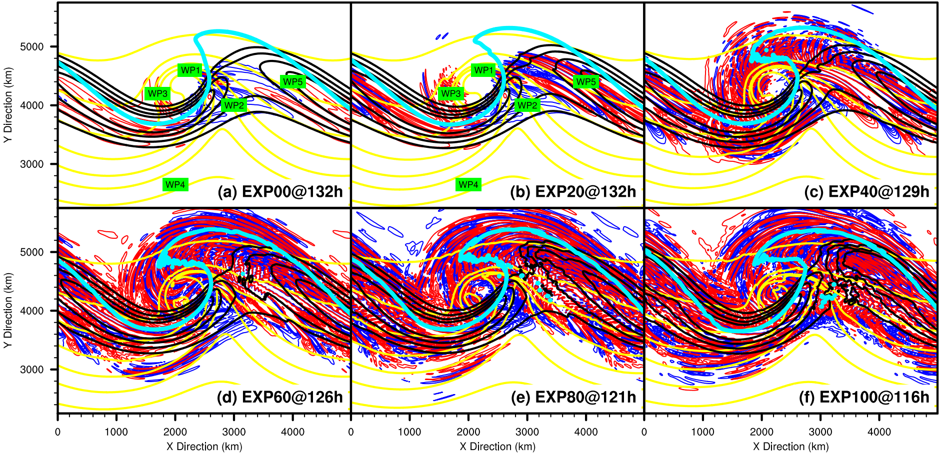

- More moisture in the initial condition suggests more energetic gravity wave field at later stage.

Part I: Motivation

- Motivated by Shutts and Vosper (2011), we seek to understand the distribution of momentum flux/drag in high-resolution idealized baroclinic wave simulations of Wei and Zhang (2014, JAS)
- The impact of gravity wave effects on the general circulation
- Potential application of gravity wave parameterizations in global models

Part II: Methodology

- How to obtain the wave-induced wind perturbation (e.g., u', w')?

A high-pass filter is applied to extract wind perturbations with wavelength below 600 km.

Part II: Methodology

- How to calculate momentum flux?

$$\rho EP_{xz} = \rho\overline{u'w'} + \frac{f}{N^2}\overline{v'b'}$$

The second term in the RHS is ignored in the current study.

The bar represents the average over one period/wavelength. In the currenty study, the bar is the spatial averaging (11-point running mean along x, then do it again along y).

Part II: Methodology

- How to calculate momentum drag?

The wave-induced forcing of the zonal mean flow is described by the divergence of the flux vector, namely

$$\frac{D\bar{u}}{Dt} - f\,\bar{v}^{*} = -\frac{1}{\rho}\frac{\partial\bar{\rho}}{\alpha x} - \frac{1}{\rho}\bigtriangledown\cdot(\rho EP_x)$$

$$EP_x = (EP_{xx}, EP_{xy}, EP_{xz})$$

In the current study, we only investigate $-\frac{1}{\rho}\frac{\partial EP_{xz}}{\partial z}$

Part III: 12-km $\overline{\rho u' w'}$ (hrz)

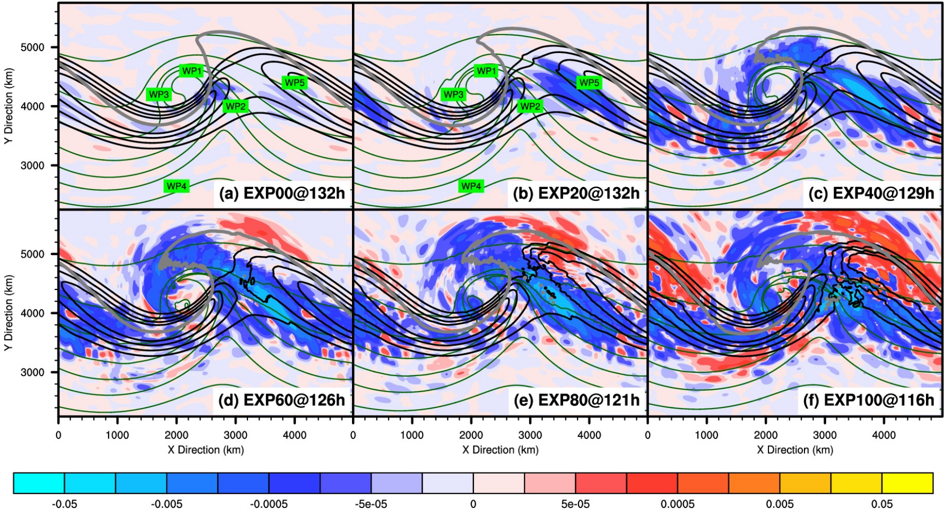

- The dominance negative values in 12-km $\overline{\rho u' w'}$

Part III: 12-km $-\frac{1}{\rho}\frac{\partial EP_{xz}}{\partial z}$ (hrz)

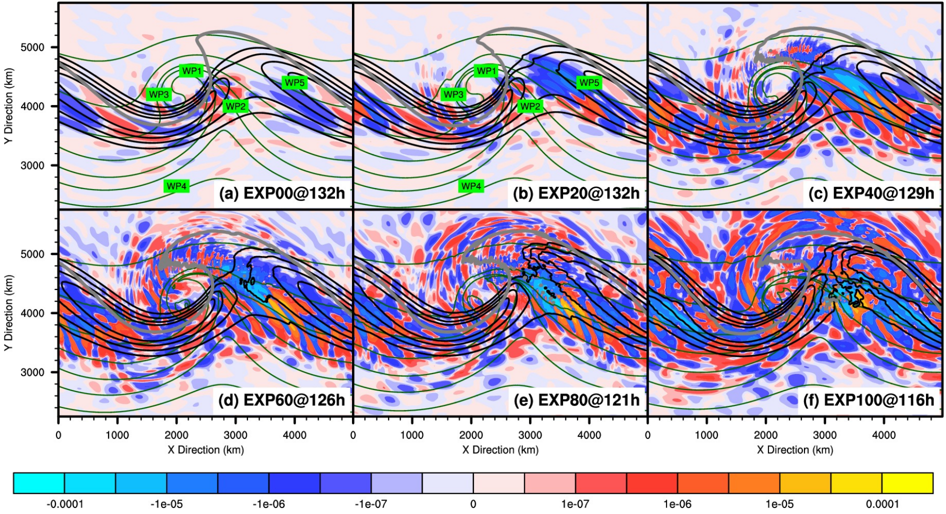

- Wave-like structure in 12-km $-\frac{1}{\rho}\frac{\partial EP_{xz}}{\partial z}$

Part III: $\rho \overline{u'w'}$ (crs)

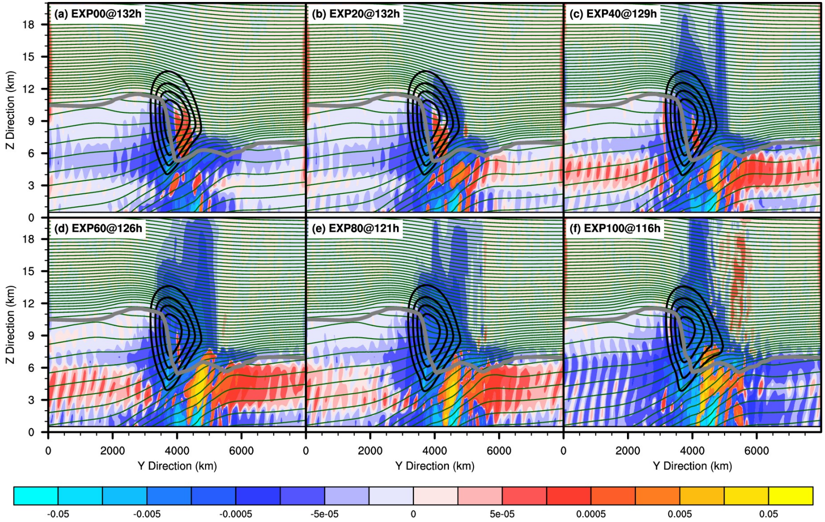

- Consistencies among all the experiments

Part III: $-\frac{1}{\rho}\frac{\partial EP_{xz}}{\partial z}$ (crs)

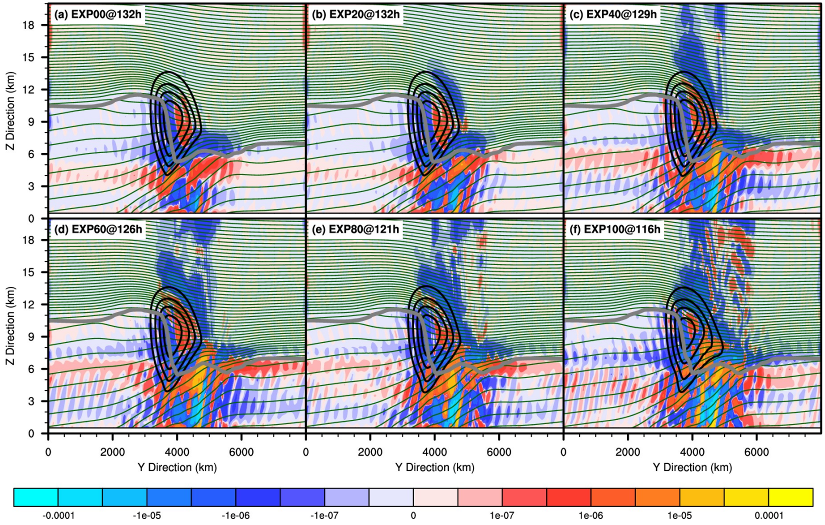

- Consistencies among all the experiments

Discussion

Eliassen and Palm (1961)

$$\overline{p'w'} = -(\bar{u} - c)\rho\overline{u'w'}$$

Case I

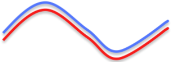

$$\overline{p'w'} > 0$$

$$\overline{u'w'} > 0 \longrightarrow c > \bar{u}$$

$$\overline{u'w'} < 0 \longrightarrow c < \bar{u}$$

Case II

$$\overline{p'w'} = 0$$

$$\overline{u'w'} = 0$$

Case III

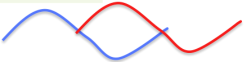

$$\overline{p'w'} < 0$$

$$\overline{u'w'} > 0 \longrightarrow c < \bar{u}$$

$$\overline{u'w'} < 0 \longrightarrow c > \bar{u}$$

- The relationship between energy flux and momentum flux is constrained by the above relationships.

Discussion

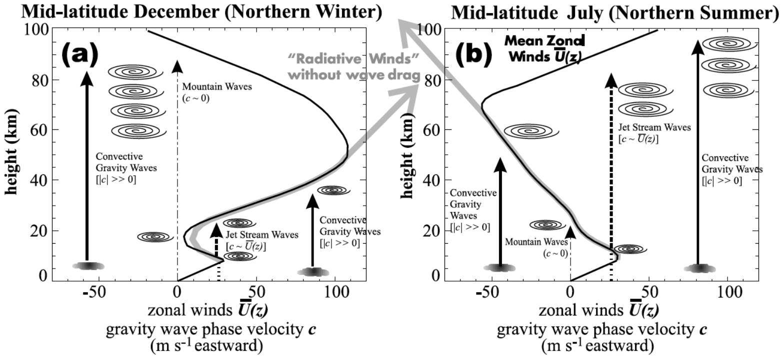

Fig. 1 Typical mid-latitude zonal winds $\overline{U}(z)$ during northern (a) winter and (b) summer. Black curve shows observed winds, grey curve shows model "radiative" winds that result without a wave drag parametrization. Sources of gravity waves with various phase speeds c are also depicted, with the source and wave breaking symbols similar to those defined in Fig. 10. On these plots, waves ascend vertically upwards since c remains constant, until they break or reach a critical level $c = \overline{U}(z_c)$. (Based on a presentation first used by Lindzen, 1981)

- The breaking levels depends on the source and the background wind, which both have seasonal variabilities. (Figure from Kim et al. 2003)

Discussion

PENNSTATE 1855

- The 12-km $\rho\overline{u'w'}$ is mostly dominated by negative values. Experiments with more initial moisture content suggest larger area of positive values.

- Compared to $\rho\overline{u'w'}$, the 12-km $-\frac{1}{\rho}\frac{\partial EP_{xz}}{\partial z}$ looks noisy, and it has wave-like structure.

- After taking averaging over one Baroclinic wavelength, there are more consistencies between $\rho\overline{u'w'}$ and $-\frac{1}{\rho}\frac{\partial EP_{xz}}{\partial z}$. There are also consistencies among all the moist runs.

- The signs of flux/drag is associated with the wave source and background flow, which both may have large seasonal variabilities.

- $\rho\overline{u'w'}$ is comparable to $\rho\overline{v'w'}$. Therefore, it is a 2D problem, instead 1D problem.